Vol. 650: 63–80, 2020
https://doi.org/10.3354/meps13396

MARINE ECOLOGY PROGRESS SERIES
Mar Ecol Prog Ser

Published September 17[§]

Contribution to the Theme Section 'Latest advances in research on fish early life stages'

Consequences of plume encounter on larval fish growth and condition in the Gulf of Mexico

Kelia E. Axler[1,4,*], Su Sponaugle[1], Frank Hernandez Jr.[2], Carla Culpepper[2], Robert K. Cowen[3]

[1]**Department of Integrative Biology, Hatfield Marine Science Center, Oregon State University, Newport, OR 97365, USA**
[2]**Division of Coastal Sciences, Gulf Coast Research Laboratory, University of Southern Mississippi, Ocean Springs, MS 39564, USA**
[3]**Hatfield Marine Science Center, Oregon State University, Newport, OR 97365, USA**

[4]***Present address:*** **Alaska Fisheries Science Center, National Oceanic and Atmospheric Administration, 7600 Sand Point Way, Seattle, WA 98115, USA**

ABSTRACT: Freshwater input into nearshore continental shelf waters from coastal river-estuarine plumes can greatly alter the physical and trophic environments experienced by fish larvae. However, the biological consequences of plume encounter on larval fish survival remain equivocal, largely due to the extreme variability of these systems but also because traditional sampling techniques alone are too coarse to effectively characterize the dynamic biophysical environment at spatiotemporal scales relevant to individual larvae. Using a multidimensional approach, we simultaneously collected *in situ* imagery and net samples of larval fishes and zooplankton from the Mobile Bay plume (Alabama, USA) and ambient continental shelf waters during a high discharge event (8–11 April 2016). We measured the effects of plume encounter on growth and condition of larval striped anchovy *Anchoa hepsetus* and sand seatrout *Cynoscion arenarius*, 2 prominent nearshore species in the northern Gulf of Mexico. Size-frequency distributions of both species indicated that larger individuals were present in shelf waters but absent from plume waters. Otolith microstructure analysis revealed that recent growth of both focal species was significantly lower for plume-collected larvae during the last few days prior to capture. Furthermore, plume larvae were in poorer morphometric condition (skinnier at length) than their shelf counterparts, despite the fact that there were higher concentrations of zooplankton prey in plume water masses. Taken together, these results suggest that elevated prey concentrations do not necessarily translate to higher growth and condition. High turbulence and turbidity within the plume may physically inhibit the prey capture ability and feeding success of fish larvae.

KEY WORDS: Ichthyoplankton · Otolith microstructure analysis · Growth · Morphometric condition · Anchovy · Seatrout

1. INTRODUCTION

In coastal river-dominated ecosystems, fisheries production is tightly linked to the prevailing hydrological and oceanographic processes that strongly regulate survival of the sensitive early life stages of fishes. River and estuarine outflow into coastal systems results in the seaward projection of a low salinity plume marked by convergent fronts with sharp density discontinuities and strong water column stratification as the buoyant plume overlies the denser (higher salinity) continental shelf waters. Within these physically dynamic and highly productive coastal ecosystems, high concentrations of larval fishes and their zooplankton prey (e.g. copepods and nauplii) have been observed in association with

*Corresponding author: kelia.axler@noaa.gov
[§] Advance View was available online August 6, 2020

freshwater plumes, particularly along plume frontal zones (e.g. Grimes & Finucane 1991, Grimes & Kingsford 1996, Cowan et al. 2008). Further, the nutrient-rich river water comprising the plume stimulates phytoplankton blooms within the nearshore continental shelf (Lohrenz et al. 1997), greatly enhancing secondary production of zooplankton (Uye et al. 1992) and creating rich feeding environments for fish larvae. Because feeding success is a major determinant of the survival and mortality of larval fishes (Blaxter 1963, Checkley 1982, Pryor & Epifano 1993), the manner in which river plumes alter the abundance and distribution of their zooplankton prey is a key process affecting fisheries recruitment.

Fish larvae and zooplankton have been observed aggregating near river and estuarine plumes and frontal systems worldwide (Le Fèvre 1987, Govoni & Grimes 1992, Kingsford & Suthers 1994, Morgan et al. 2005, Peterson & Peterson 2008), thus larval fish encounters with these dynamic coastal features is presumed to be beneficial (e.g. more feeding opportunities). For instance, if fish larvae encounter their zooplankton prey more frequently within these plume-derived aggregations, feeding success may be higher relative to non-plume environments. Faster-growing fish larvae in better body condition often have improved swimming capabilities (Grorud-Colvert & Sponaugle 2006) and consequently higher survival (Houde 1987, 2009, Anderson 1988). However, the biological consequences of such aggregations for fish larvae (e.g. faster growth, higher condition index) are neither clear nor consistent across the literature. In some systems, previous studies have reported faster growth for plume-associated fish larvae relative to conspecifics captured outside of the productive plume region (Grimes & Lang 1992, Lang et al. 1994, Rissik & Suthers 1996). However, the degree to which plume encounters convey a survival advantage to the larval stages is unclear, with other studies finding that plume-associated larvae had slower growth rates and no dietary or survival advantages (Govoni & Chester 1990, Powell et al. 1990, Lochmann et al. 1997, Allman & Grimes 1998). Therefore, river plumes appear to have a major, though variable, effect on the number of larval fishes that survive to recruit to coastal marine fish populations (Sabatés & Masó 1990). Some of the conflicting findings may be due to the highly dynamic nature of river plumes and the lack of sampling methodologies that can adequately capture these dynamics. For instance, convergent plume fronts can persist over time scales of several tidal cycles (hours) to several days, depending on the magnitude of river discharge, shelf circulation, and local wind stress (Dinnel et al. 1990). Though brief, these temporal scales are long enough to affect larval fish feeding, condition, growth, and ultimately survival to the adult stages if the feeding environment changes from favorable to poor (e.g. dispersal of a localized aggregation of prey).

Recently, high-resolution sampling of a 2-layer system (low-salinity plume at the surface overlying high-salinity shelf water at the bottom) has enabled observations of fine-scale (1 m) biological distributions in response to broad-scale (10s of km) physical forcing across multiple pulses of plume water in the northern Gulf of Mexico (Fig. 1A; Axler et al. 2020, this Theme Section). A plankton imaging system towed through plume water emanating from the mouth of Mobile Bay documented fish larvae and zooplankton aggregating in a plume-derived convergent region on the nearshore Alabama (USA) continental shelf during calm wind conditions (Fig. 1C; Axler et al. 2020). Over the following 2 d, however, strong wind-driven turbulence and mixing rapidly dissipated the aggregation, separating fish larvae from their zooplankton prey. Axler et al. (2020) concluded that in stable conditions, the high productivity and physical retention mechanisms (e.g. aggregation via hydrodynamic convergence) inherent to a river-influenced coastal region should enhance larval fish survival via bottom-up processes (i.e. increased prey contact and feeding). However, if physical forcing of the system becomes too strong (e.g. via wind-stress in conjunction with high river discharge) and begins to dominate biological interactions (i.e. via spatial separation of fish larvae from their prey), the habitat can quickly become unfavorable for larval fishes.

In the present study, we examined whether entrainment, or the process of larvae being drawn into and transported by these dynamic plumes with elevated prey concentrations, leads to faster growth and higher condition of fish larvae. We selected 2 common nearshore fish species, striped anchovy *Anchoa hepsetus* (Engraulidae) and sand seatrout *Cynoscion arenarius* (Sciaenidae) and used otolith microstructure and body morphometric analyses to examine variation in size and age distributions, growth, and condition of plume-entrained larvae relative to those sampled from the nearshore Alabama continental shelf. While the focus of the present study is on the growth and condition of these fish larvae, we include a brief summary of the physical conditions within the Mobile Bay plume and surrounding waters that are reported in greater detail in a companion paper (Axler et al. 2020). The combination of these growth

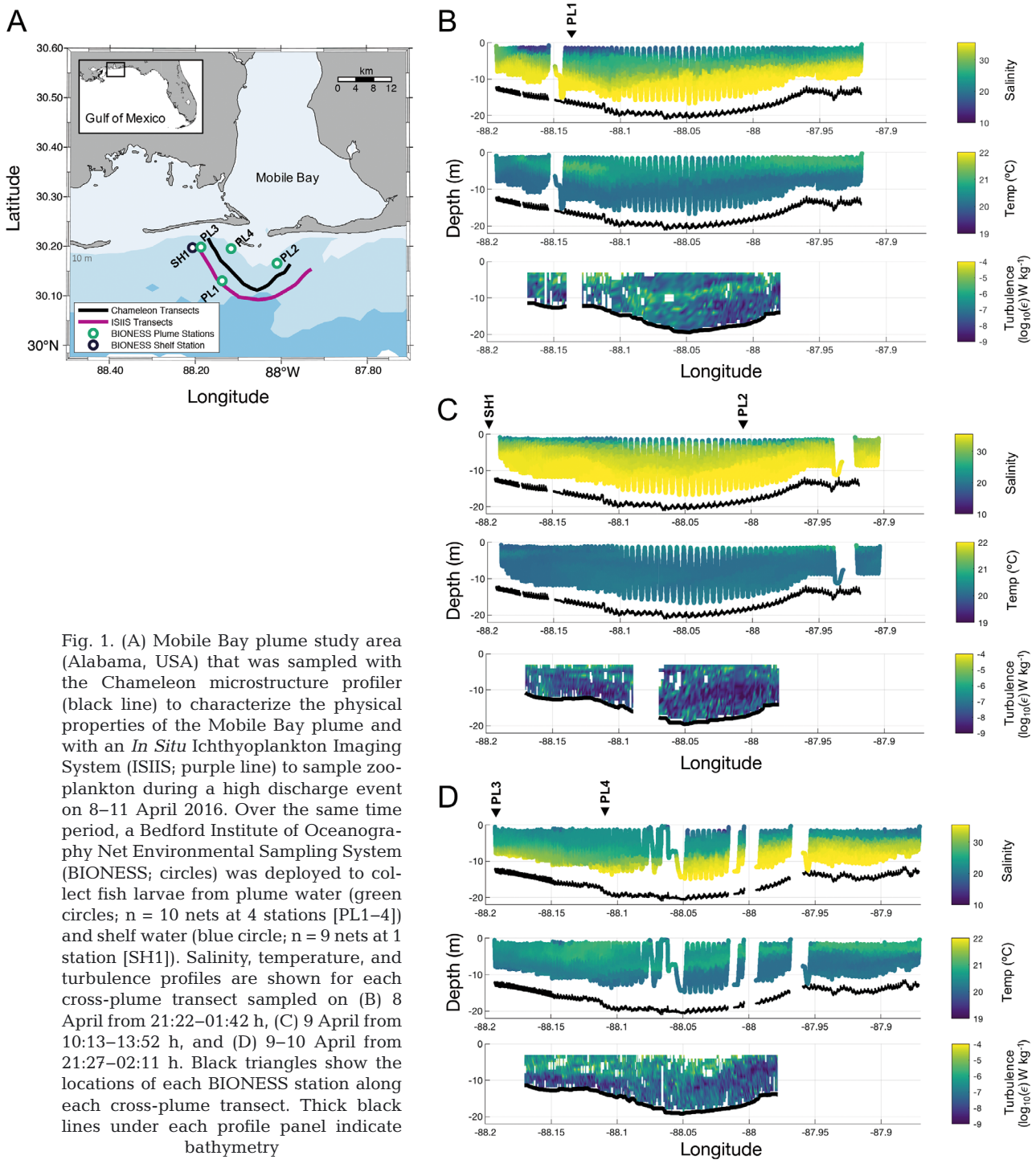

Fig. 1. (A) Mobile Bay plume study area (Alabama, USA) that was sampled with the Chameleon microstructure profiler (black line) to characterize the physical properties of the Mobile Bay plume and with an *In Situ* Ichthyoplankton Imaging System (ISIIS; purple line) to sample zooplankton during a high discharge event on 8–11 April 2016. Over the same time period, a Bedford Institute of Oceanography Net Environmental Sampling System (BIONESS; circles) was deployed to collect fish larvae from plume water (green circles; n = 10 nets at 4 stations [PL1–4]) and shelf water (blue circle; n = 9 nets at 1 station [SH1]). Salinity, temperature, and turbulence profiles are shown for each cross-plume transect sampled on (B) 8 April from 21:22–01:42 h, (C) 9 April from 10:13–13:52 h, and (D) 9–10 April from 21:27–02:11 h. Black triangles show the locations of each BIONESS station along each cross-plume transect. Thick black lines under each profile panel indicate bathymetry

data with the detailed description of the complex environmental setting (*in situ* water column properties, wind-stress, and physical forcing of the plume) and fine-scale biological responses (plankton distributions, predator–prey relationships) enables a thorough examination of the effects of plume encounter on larval fish growth and condition at very fine spatial and temporal scales.

2. MATERIALS AND METHODS

2.1. Study region and plume sampling

Mobile Bay (Alabama, USA) is a shallow, river-dominated estuary in the northern Gulf of Mexico that discharges pulses of freshwater that vary in size and seasonal flow and drive a salinity gradient

between the bay mouth and coastal shelf waters. It is the largest local system delivering freshwater to the Mississippi Bight (Greer et al. 2018) and the fourth largest river system in the continental USA (Schroeder & Lysinger 1979), with a long-term (1976–2011) daily mean discharge of 2656 $m^3 s^{-1}$ during the spring season that forms a sizable plume (Dzwonkowski et al. 2014). To capture the biological effects of entrainment within a low-salinity plume on individual fish larvae, we sampled the Mobile Bay plume and adjacent shelf waters during a high discharge event (8–11 April 2016; >4500 $m^3 s^{-1}$; Dinnel et al. 1990). Distinctive Mobile Bay plume signatures were identified by a suite of oceanographic equipment (see Greer et al. 2018, Axler et al. 2020), including the Chameleon microstructure profiler (Moum et al. 1995). The Chameleon microstructure profiler was towed east to west in an arc behind the RV 'Pelican' over 3 transects (~25 km in length) approximately 10 km south of Mobile Bay at sampling depths between 10 and 20 m to sample water column fluorescence, microstructure turbulence, temperature, optical backscatter (800 nm), and conductivity (Fig. 1A). All Chameleon measurements extended from the surface to within 2 cm of the bottom except turbulence, which was contaminated by instrument vibration in the upper 4 m. Because of this contamination, turbulence dissipation values <4 m were not plotted. It is therefore likely that higher values of turbulence dissipation would have been measured if we had been able to more thoroughly sample the shallow plume waters (i.e. those above 4 m in depth; Fig. 1D).

2.2. Ichthyoplankton collection

Striped anchovy and sand seatrout larvae were sampled at 5 nearshore stations (within 15 km of the Alabama coastline) near the mouth of Mobile Bay on 8–10 April 2016 using a multinet Bedford Institute of Oceanography Net Environmental Sampling System (BIONESS) sampler (Open Seas Instrumentation) towed from a second ship, the RV 'Point Sur' (Fig. 1A). The 0.25 m^2 mouth opening of the BIONESS was fitted with 333 µm mesh nets (n = 6) and 202 µm mesh nets (n = 3), although fish larvae were utilized from all nets regardless of mesh size to ensure adequate sample sizes. Tows were conducted during both daylight and nighttime hours. The BIONESS was outfitted with a conductivity-temperature-depth probe (CTD; SBE19, Sea-Bird Electronics) to provide temperature (°C), salinity (unitless), and depth (m) profiles for each tow. Mean temperature and salinity observations (average of values measured at the opening and closing time of the nets for each depth bin) were examined at each station to determine the real-time environmental conditions in which larval fishes were collected. A flowmeter was used (General Oceanics) to calculate the volume filtered for each sample. Plankton net contents were rinsed with seawater, sieved, fixed in 95% ethanol, and stored in 85% ethanol. All fish larvae collected by the BIONESS nets were sorted and identified to the lowest possible taxonomic level, and striped anchovy and sand seatrout were separated out for further analyses. Concentrations of each species (ind. m^{-3}) were calculated by dividing counts from each net by the volume of water filtered through the net.

Because salinity gradients were consistent with other plume characteristics in delineating the general boundaries of each plume water mass (e.g. fluorescence, temperature, dissolved oxygen, and turbulence; Axler et al. 2020), low salinity (≤25) was used as an indicator of the Mobile Bay plume. Although the plume tended to fluctuate in magnitude of river discharge and spatial extent, 4 of the net stations sampled low-salinity (≤25) plume waters (Fig. 1A, PL1–4) while a fifth station sampled the higher-salinity Gulf of Mexico 'shelf' water underlying a shallow (<2 m) surface plume approximately 15 km to the west of Main Pass (Fig. 1A, SH1). This shelf station was sampled to target 'non-plume' fish larvae for comparison with conspecifics captured from directly within the plume. Because plume water masses were intrinsically shallower than shelf waters (due to the buoyancy of low-salinity water), only shelf net samples ≤10 m depth were analyzed to standardize depth between plume and shelf stations (for specific depths sampled at each station, see Table S1 in the Supplement at www.int-res.com/articles/suppl/m650p063_supp.pdf). Based on the designated salinity and depth criteria, 10 plume net samples and 9 shelf net samples were selected for analysis. These samples were used to provide specimens for growth and morphometric condition analyses (Table S2).

2.3. Zooplankton imagery collection and image processing methodology

Three-dimensional water column plankton imaging was conducted along transects near the Mobile Bay plume outflow immediately preceding and following ichthyoplankton sampling (via BIONESS net tows) to examine zooplankton distributions and concentrations in plume and shelf waters. A plankton

shadowgraph imager (*In Situ* Ichthyoplankton Imaging System, ISIIS; Cowen & Guigand 2008) was towed in a parallel transect ~3 km downstream (south) of the Chameleon profiler from the RV 'Point Sur,' over 3 transects approximately 10–15 km south of Mobile Bay sampling depths between 10 and 20 m (Fig. 1). ISIIS uses motor-actuated wings to undulate through the water column within ~1 m of the surface to ~2 m from the bottom at horizontal speeds of ~2.5 m s^{-1} and vertical speeds of 0.2–0.3 m s^{-1}, all while imaging large volumes of water (150–185 l s^{-1}; Cowen et al. 2013) with 2 line-scan cameras to capture zooplankton ~500 µm to 12 cm in length. ISIIS was also outfitted to simultaneously measure salinity, temperature, and depth (Sea-Bird Electronics 49 FastCAT), dissolved oxygen (SBE 43), chlorophyll *a* fluorescence (Wet Labs FLRT), and photosynthetically active radiation (PAR; Biospherical QCP-2300) while collecting *in situ* images of planktonic organisms around the Mobile Bay plume.

Zooplankton taxa were sorted into image classes based on taxonomy and morphology using an automated algorithm, flat-fielded and segmented to regions of interest, and classified using a sparse convolutional neural network as described by Axler et al. (2020). Calanoid copepods were selected as the representative zooplankton prey group from the ISIIS images because of their documented prevalence as a major dietary component of both larval striped anchovy and sand seatrout in this region during the time period of the study (Axler 2019) as well as in the literature (McNeil & Grimes 1995, Holt & Holt 2000). The ISIIS imagery was grouped by plume (salinity ≤25) or shelf (non-plume) water, and concentrations (ind. m^{-3}) of 1 m vertically binned calanoid copepods were compared across plume and shelf water masses for each transect.

Diagnostic plots of residuals of larval fish and zooplankton concentration data were examined to assess the normality of distributions and homoscedasticity of variances using R (v3.4.1, R Core Team 2019). Histograms and residual quantile-quantile plots showed that concentrations of striped anchovy, sand seatrout, and calanoid copepods between water masses had non-normal distributions and unequal variance. Log-(x + 1)-transformations applied to the concentration data achieved near-normality of distributions of all taxa. However, the transformations did not greatly improve the spread of the residuals across the fitted values due to the relatively heterogeneous variance, and thus taxa concentrations were compared between plume and shelf water masses using Welch's *t*-tests (R Core Team 2019). All data visualization was performed in R (R Core Team 2019) using the packages 'dplyr' (Wickham et al. 2018) and 'ggplot2' (Wickham 2016).

2.4. Size and growth analysis

Larval striped anchovy and sand seatrout body lengths were measured to the nearest 0.01 mm (either notochord length if pre-flexion or standard length [SL] if post-flexion) using a Leica MZ16 dissecting microscope. All plume specimens were measured for both species (striped anchovy: n = 115, sand seatrout: n = 145), and a random subsample of shelf larvae was measured for comparison (striped anchovy: n = 187, sand seatrout: n = 221). All imaging was conducted using a QImaging digital camera and Image-Pro Premier 9.1 software (Media Cybernetics). Otolith microstructure analysis was used to obtain age distributions for both striped anchovy and sand seatrout. Random subsamples of ≥50 individual seatrout in the 2–4 mm SL size class were selected from each water mass for otolith microstructure analyses. Similarly, ≥50 individual anchovies in the 7–20 mm range were selected from each water mass depending on sample availability. Due to sample size constraints, examination of growth and condition at the level of individual stations was not possible and thus fish larvae were pooled by plume or shelf stations. Sagittal otoliths were dissected from each individual and stored in immersion oil on a glass slide for a week to 'clear' and facilitate reading (Sponaugle et al. 2009). All otoliths from both species were read twice blind (without knowledge of previous readings, dates, or fish sizes) by a single reader. Otoliths were read along the longest axis at 1000× magnification through a Zeiss Axio Scope.A1 compound microscope using a QImaging digital camera and Image-Pro Plus software. If the 2 reads differed by ≤5%, 1 read was randomly chosen for analysis. If reads differed by >5%, a third read was conducted and compared with the first 2 reads. If any comparison differed by ≤5%, 1 read from that comparison was randomly chosen for analysis. Otoliths where all reads differed by >5% were removed from any further analyses (Sponaugle et al. 2009).

Two separate otolith microstructure analyses were used to compare the variation in larval growth of the focal species captured in plume and shelf water masses: (1) recent growth and (2) daily otolith growth (mean increment widths, MIWs, for each day of life) as a proxy for growth at specific ages during larval life. Because the exact timing of larval entrainment

within a plume could not be determined, we examined recent growth during the last 3 complete days prior to capture for all larvae to minimize the potential effect of differential spatial and environmental conditions on early larval growth. Otolith increment width increases with the age of the individual fish, so we corrected for this by detrending for age (e.g. Baumann et al. 2003, Robert et al. 2009). Detrending for age enabled us to compare recent growth of differently aged larvae. A detrended growth index was computed using:

$$DG_{ij} = (G_{ij} - G_j)\, SD_j^{-1} \quad (1)$$

where DG_{ij} is the detrended growth of the individual i at age j, G_{ij} is the otolith growth (increment width) for individual i at age j, G_j is the mean of otolith growth of all individuals at age j, and SD is the standard deviation of G (Robert et al. 2009). The detrended growth index was computed for the last 3 full days of life for each fish larva (i.e. width of the last 3 complete otolith increments). We then compared the mean detrended recent growth (DRG) for each species from the 2 water mass types using analysis of covariance (ANCOVA) with age as a covariate. The oldest (>14 d) and youngest (<7 d) *Cynoscion arenarius* (n = 42 or 25%) were removed from analyses due to uneven sample sizes between water masses. The effect of temperature on DRG was also assessed using linear regression.

Linear mixed effects models (LMMs) were used to test whether mean daily growth differed between plume- and shelf-captured fish larvae for each of the 2 species. The model parameters for each species included the fixed effects of water mass (plume or shelf), age, and a water mass × age interaction term. Fish identity was used in all models as the random effect term to account for repeated measures of daily growth of individual fish. First-order autoregressive correlation terms were also included in all models to account for the inherent autocorrelation between sequential otolith increments (Weisberg et al. 2010). Model selection was performed using a backward stepwise approach. The full model introduced both a random intercept term (fish identity) and a random slope term (age) for each individual, which was compared to reduced models that successively removed random and fixed effects (Table 1). The full and reduced versions of the models were then compared using Akaike's information criterion (AIC) as a measure of goodness of fit, and the best model was identified for each species by minimizing AIC (Table 1; Burnham et al. 2002). For both striped anchovy and sand seatrout, the model that best fit the daily growth trajectory included both the random intercept and slope terms for each individual. The full models used to test for differences in daily growth of both species between plume and shelf water masses had the form:

$$y_{i,w,a} = \alpha_w + \beta_w \text{age} + a_i + b_i \text{age} + \varepsilon_{i,w,a} \quad (2)$$

where $y_{i,w,a}$ is the growth increment or size of individual i of water mass w (plume or shelf) at age a; α_w and β_w are the overall intercept and slope of the daily growth trajectory; a_i and b_i are the random intercept and slope for individual i; and $\varepsilon_{i,w,a}$ is a residual that is assumed to follow a first-order autoregressive process: $\varepsilon_{i,w,a} = \Phi\varepsilon_{i,w,a-1} + \nu_{i,w,a}$ where Φ is the autoregressive coefficient and $\nu_{i,w,a}$ is a normally distributed residual with mean 0 and variance σ_ν^2. The random effects a_i and b_i are assumed to be normally distributed with zero means, variances σ_a^2 and σ_b^2, and covariance $\sigma_{a,b}$. Model diagnostics and residuals were checked for potential deviations from the assumptions of normality and homogeneity of variance. All models were coded in R software (R Core Team 2019), and the final growth parameters were esti-

Table 1. Model selection for mean daily growth trajectories of larval striped anchovy and sand seatrout. Fixed effects are listed on the left of the vertical line and random effects are to the right. AIC: Akaike's information criterion; the lowest AICs were 1198.87 (striped anchovy) and 206.55 (sand seatrout)

Striped anchovy	Δ AIC
Water mass + Age + Water mass × Age | Random intercept + Random slope + Auto Correlation	0
Water mass + Age + Water mass × Age | Random intercept + Auto correlation	44.36
Water mass + Age + Water mass × Age | Auto correlation	42.36
Water mass + Age | Auto correlation	65.42
Water mass | Auto correlation	528.38
Null model	7152.65
Sand seatrout	**Δ AIC**
Water mass + Age + Water mass × Age | Random intercept + Random slope + Auto correlation	0
Water mass + Age + Water mass × Age | Random intercept + Auto correlation	105.71
Water mass + Age + Water mass × Age | Auto correlation	106.29
Water mass + Age | Auto correlation	134.27
Water mass | Auto correlation	907.09
Null model	3393.50

mated using restricted maximum likelihood with the R package 'nlme' (Pinheiro et al. 2019). Only MIW values that allowed for a minimum of n = 4 observations per day per group were analyzed (MIW values were truncated when sample sizes of fishes per day per water mass were n < 4).

2.5. Morphometric condition analysis

To examine differences in larval fish body condition between plume and shelf water masses, we analyzed larval morphology using 5 linear body dimensions (6 for seatrout larvae) that have been shown in other species to vary with larval feeding success, and hence are related to body condition (body depth at pectoral fin, DPF; body depth at anus, DA; head length, HL; head depth, HD; eye diameter, ED; and in the case of seatrout, lower jaw length, LJL; Lochmann & Ludwig 2003, Gisbert et al. 2004, Hernandez et al. 2016, Ransom et al. 2016). In general, deeper-bodied and heavier larvae at a given length are in better condition than their skinnier counterparts. Only specimens with the full suite of morphometric measurements were used in the analysis of body condition. The residual of each body measurement (e.g. head depth) was computed from its linear correlation with notochord length to standardize and account for size variation among larvae (Hernandez et al. 2016). We did not correct for ethanol shrinkage because of the relatively narrow size range of collected specimens (8–18 mm for striped anchovy and 2–7 mm for sand seatrout); however, to be conservative, we conducted 2 analyses: (1) on all fish larvae and (2) on a size-truncated portion of the collected specimens of both species. The size-truncated analyses were conducted to account for the larval size differences between water masses as well as the potential influence of allometric and ontogenetic changes in body morphology that occur during the transition from pre- to post-flexion larval stages (Suthers 1998). Flexion in striped anchovy occurs at ~8–9 mm (Richards 2005) and therefore larvae <10 mm and >16 mm (n = 24) were removed from the size-truncated analysis to examine the morphometrics of a narrower size range of post-flexion larvae. Similarly, flexion in sand seatrout occurs at ~4.2–5.2 mm (Richards 2005), thus larvae >4 mm (n = 11) were removed from the corresponding size-truncated analysis to examine only pre-flexion larvae.

Nonmetric multidimensional scaling (NMS) was used to ordinate larvae according to body shape to investigate changes in morphometric condition between water masses (Kruskal 1964, Mather 1976). NMS ordination was chosen for the morphometric analyses because it accounts for the high degree of correlations among the different body dimensions and also because it has the least restrictive assumptions and can represent the structure of data sets in their original dimensions (McCune et al. 2002). All NMS ordinations were performed in PC-ORD version 7 software (McCune et al. 2002; MjM Software Design). The final NMS ordination was performed using the 'slow and thorough' autopilot setting in conjunction with the Sorensen Bray-Curtis distance measured on the residual body dimensions. A nominal value of 1 was added to all residuals because the Bray-Curtis distance measure can only calculate distances for positive integers. Outliers were identified as those larvae with an average distance of >3 SDs above the grand mean of distances and removed from the analysis (n = 3 striped anchovy larvae and n = 5 sand seatrout larvae). Once the NMS axes were derived, each axis was correlated with the original body dimension residuals to identify which dimensions appeared to drive variation among larval body shape (Hernandez et al. 2016). NMS axes were independently analyzed to compare differences in larval body shape because they are orthogonal (Rettig et al. 2006). For both species of fish, Axis 1 explained most of the variation in body shape and thus non-parametric Mann-Whitney *U*-tests were applied to Axis 1 scores to determine differences among larvae collected from plume and shelf water masses using R (R Core Team 2019).

3. RESULTS

3.1. Environmental setting and biological concentrations

Over the study period of 8–11 April 2016, a brackish (salinity ~10 to 25) plume emanated from the mouth of Mobile Bay across the Alabama continental shelf (Fig. 1B). Sharp density discontinuities delineated the general boundaries of the plume and were consistent with lower salinity (yet higher fluorescence and dissolved oxygen; see Axler et al. 2020) than the underlying shelf water (Fig. 1B–D). In general, Mobile Bay plume water was slightly warmer (≥20.8°C on average) than the underlying coastal shelf water (≤20.3°C), although temperature varied little overall (<1°C; Fig. 1B–D). Most notably, turbulence dissipation was measured to be at least an order of magnitude higher on average in the plume

(3.7×10^{-6} W kg^{-1}) than in the underlying shelf water (7.1×10^{-7} W kg^{-1}; Fig. 1B,C).

A total of 2903 fish larvae net-captured during our study period could be identified to family. The total concentrations of fish larvae (mean ± SD number of ind. m^{-3}) did not vary significantly between plume (0.297 ± 0.403 ind. m^{-3}) and shelf stations (0.413 ± 0.453 ind. m^{-3}) within the study region (log(x + 1)-transformed, Welch's test: t = 1.47, df = 116.34, p = 0.143). Families Engraulidae and Sciaenidae comprised 74.4 and 23.9% of the total fish larvae, respectively, with striped anchovy and sand seatrout dominating their respective families. In total, 372 striped anchovy and 475 sand seatrout were collected during this study. Concentrations of larval striped anchovy were highly variable and did not differ significantly between plume (0.401 ± 0.333 ind. m^{-3}) and shelf stations (0.566 ± 0.233 ind. m^{-3}; log(x + 1)-transformed, Welch's test: t = 1.12, df = 12.46, p = 0.284). However, there were significantly lower concentrations of sand seatrout in plume (0.195 ± 0.208 ind. m^{-3}) than in shelf water masses (0.605 ± 0.368 ind. m^{-3}; log(x + 1)-transformed, Welch's test: t = 2.91, df = 12.64, p = 0.012).

Fine-scale ISIIS sampling found significantly more calanoid copepods, a major prey group of both larval striped anchovy and sand seatrout, in plume waters than in adjacent shelf waters on 9 April (Fig. 2; log(x + 1)-transformed, Welch's tests: t = −11.40, df =

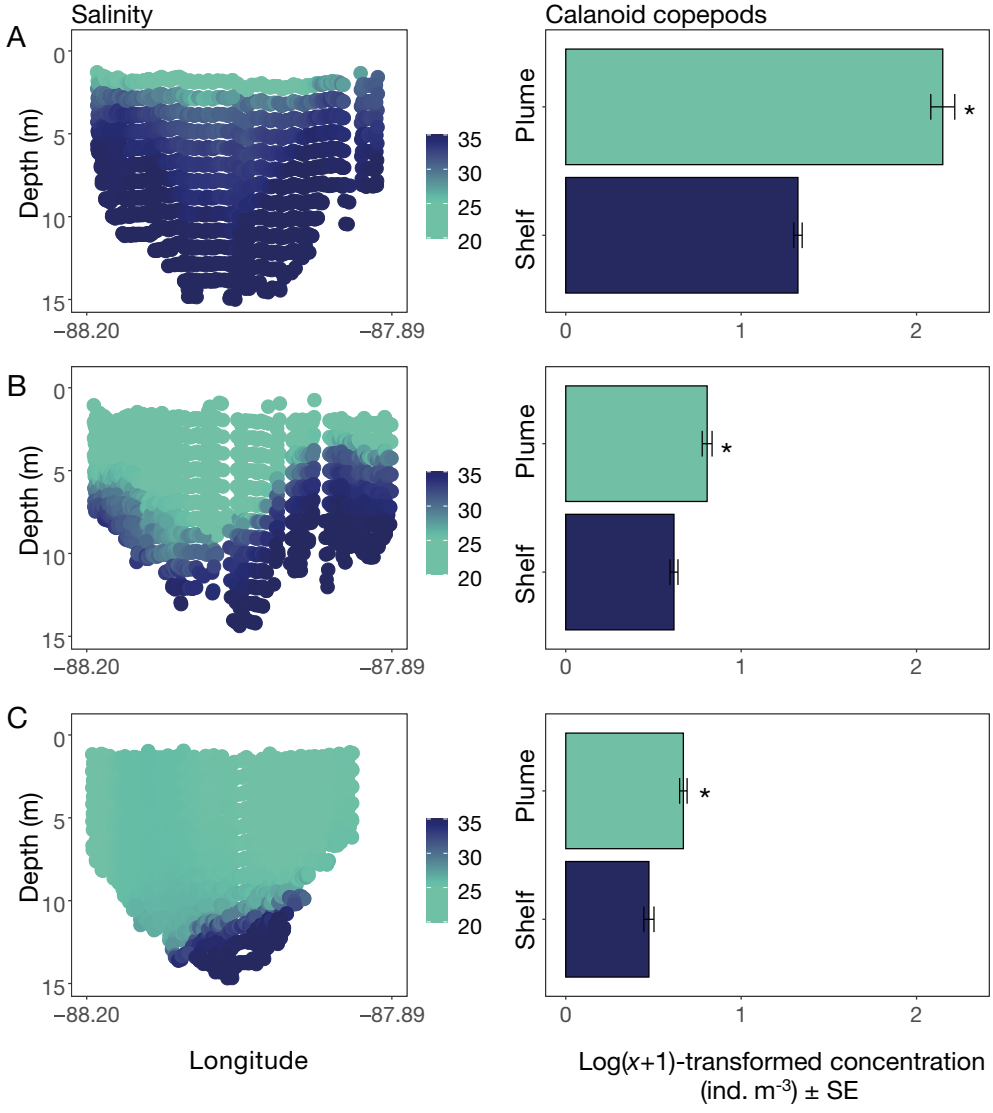

Fig. 2. Log(x + 1)-transformed mean ± SE concentration (ind. m^{-3}) of calanoid copepods per 1 m depth bin in cross-plume transects near the mouth of Mobile Bay on (A) 9 April, (B) 9–10 April, and (C) 10–11 April, with salinity profiles shown in the left panels. All physical and biological data were collected by the ISIIS. Asterisks indicate significant differences between water masses (Welch's t-tests: p < 0.01)

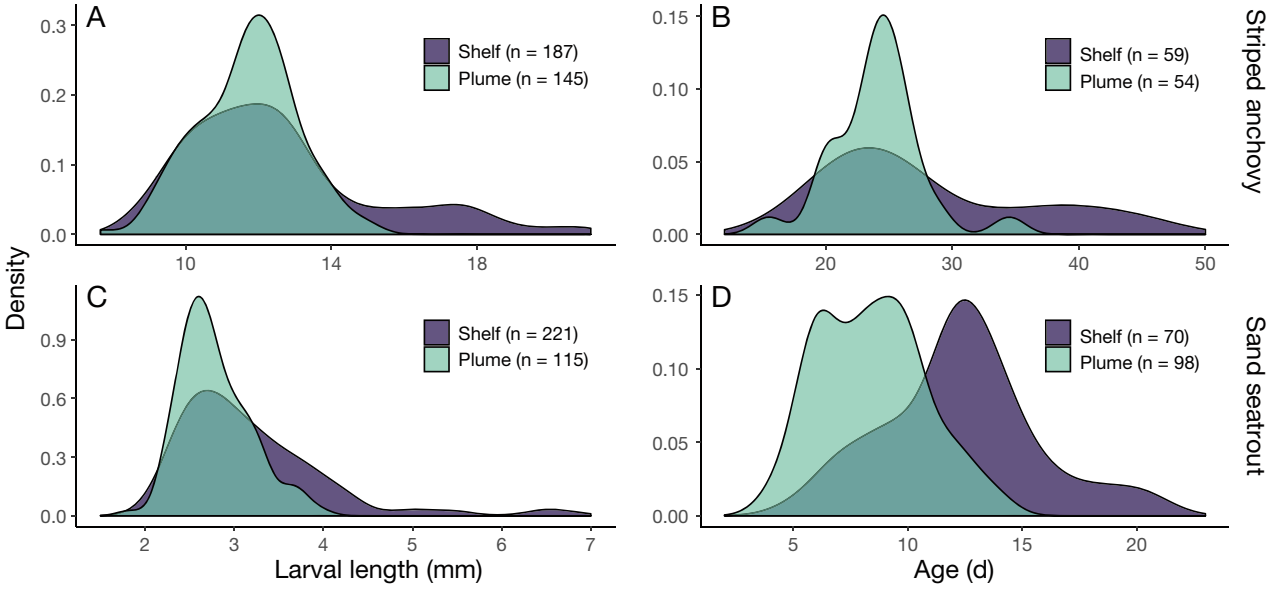

Fig. 3. Kernel density estimates of size and age distributions between plume (green) and shelf (blue) collections of (A,B) striped anchovy *Anchoa hepsetus* and (C,D) sand seatrout *Cynoscion arenarius*. Note that axes differ between species. Sample sizes (n) are listed next to each plot

180.43, $p < 0.0001$), 9–10 April ($t = -5.23$, df = 1907.7, $p < 0.0001$), and 10–11 April ($t = -9.96$, df = 1804.4, $p < 0.0001$).

3.2. Size and growth analysis

Both striped anchovy and sand seatrout showed variable size and age distributions between water masses. Striped anchovy larvae ranged in size from 7 to 21 mm SL and were 15 to 47 d old. Sand seatrout larvae were 1 to 7 mm SL and were 4 to 21 d old. Size- and age-frequency distributions revealed that relatively larger (>15 mm) and older (>37 d) anchovy and seatrout (>3.5 mm and >16 d) larvae were present in shelf waters but absent from plume waters (Fig. 3). Recent growth was used to analyze the potential effects of residence in different environmental conditions on growth rate over the last few days prior to collection. Mean DRG during the last 3 full days of life was significantly slower in plume than in shelf water masses for both striped anchovy (ANCOVA: $F_{2,110} = 3.499$, $R^2 = 0.598$ $p = 0.033$) and sand seatrout (ANCOVA: $F_{2,123} = 2.982$, $R^2 = 0.046$, $p = 0.017$; Fig. 4). Temperature varied by <1°C between plume and shelf waters, and there was no sig-

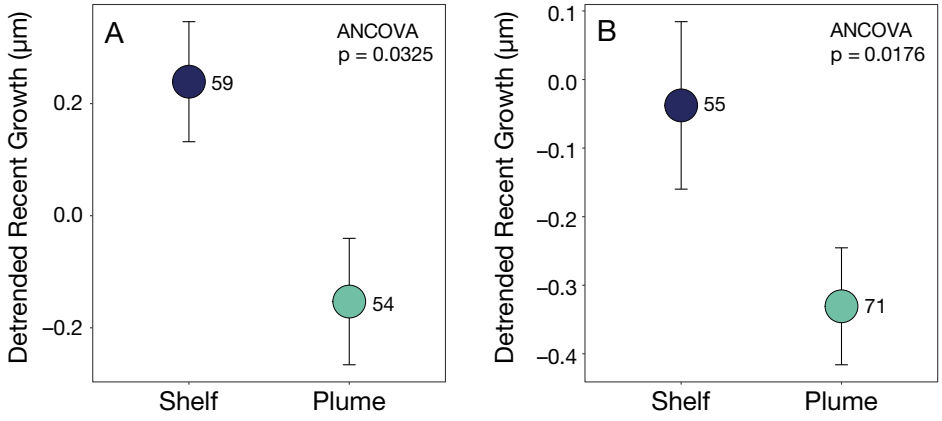

Fig. 4. Mean ± SE detrended mean recent growth (DRG) of the last 3 complete days of life prior to collection for larval (A) striped anchovy and (B) sand seatrout captured from either plume (green) or shelf (blue) water masses. Analysis of covariance (ANCOVA) with age as a covariate was used to compare recent growth between plume and shelf habitats. Sample sizes of fish larvae are denoted next to each datum. Note that *y*-axes differ between species

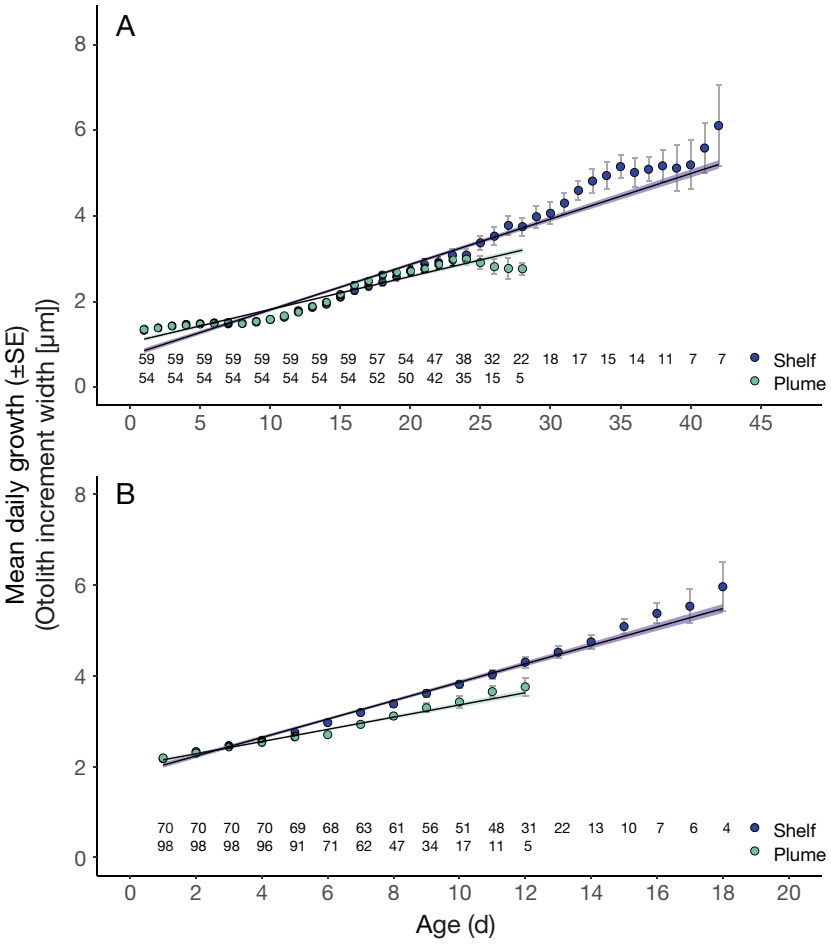

Fig. 5. Mean (±SE) daily growth for (A) striped anchovy and (B) sand seatrout larvae collected from plume and shelf water masses. Otolith mean increment width (MIW) values were truncated when n < 4. Fitted lines represent the linear mixed effects models for each trajectory. Shaded area surrounding lines indicate 95% CI. Sample sizes (n) for every other increment (A) or every increment (B) are indicated at the bottom of each plot

nificant relationship between recent growth and temperature for either larval striped anchovy ($F_{1,111}$ = 1.21, p = 0.275, R^2 = 0.011) or sand seatrout ($F_{1,166}$ = 0.366, R^2 = 0.002, p = 0.546).

Daily growth as measured by otolith MIWs varied significantly with age and water mass occupied by the larvae (Fig. 5). For both species, LMMs indicated that MIW was initially slightly higher for plume larvae than shelf larvae in early life but then reversed (~15–25 d for larval anchovy and ~5–6 d for larval seatrout) and began increasing more rapidly with age in shelf larvae than plume larvae (Fig. 5). For larval anchovy, MIW was significantly affected by water mass, age, and the age × water mass interaction (LMM: p < 0.01; Table 2). In comparison, MIW of larval seatrout was not significantly affected by water mass (LMM: p = 0.086); however, both age and the age × water mass interaction did affect MIW (LMM: p < 0.0001; Table 2).

3.3. Morphometric condition analysis

Among the focal specimens collected, 106 striped anchovy and 182 sand seatrout met the criteria for morphometric condition analyses. The NMS ordination performed on the

Table 2. Linear mixed effects model results for mean daily growth of larval striped anchovy and sand seatrout with 95% confidence interval estimates and p-values for each fixed effect, standard deviations (SD) for random effects and residuals, and magnitude of the auto-regressive coefficients (Φ). **Bold** p-values are significant (p < 0.05)

Parameter	Lower bound	Estimate	Upper bound	p	Random effect	SD	Φ
Striped anchovy							
Intercept	0.754	0.876	0.999	**<0.0001**	Intercept	0.040	0.841
Water mass	0.088	0.271	0.455	**0.0041**	Slope (Age)	0.023	
Age	0.094	0.103	0.112	**<0.0001**	Residuals	0.529	
Water mass × Age	−0.045	−0.030	−0.016	**<0.0001**			
Sand seatrout							
Intercept	1.866	1.930	1.995	**<0.0001**	Intercept	0.022	0.596
Water mass	−0.012	0.078	0.167	0.0878	Slope (Age)	0.044	
Age	0.170	0.184	0.197	**<0.0001**	Residuals	0.293	
Water mass × Age	−0.061	−0.040	−0.020	**0.0001**			

residuals of the 5 linear body dimensions of striped anchovy resulted in a 2-dimensional solution that explained 91.2% of the variation in the larval morphometric measurements (final stress = 13.70948 and instability <0.000001 after 107 iterations of real data). Axis 1 explained 71.8% of the variation in larval body shape, while Axis 2 explained an additional 19.4%. A similar NMS ordination on the residuals of 6 body dimensions of sand seatrout larvae settled on a 2-dimensional solution that explained 96.2% of the variation in the larval morphometric measurements (final stress = 9.98360 and instability <0.000001 after 65 iterations of real data). Axis 1 explained 88.3% and Axis 2 explained 7.8% of the data.

For both species of fish, Axis 1 explained most of the variation in body shape. Axis 1 scores were strongly and positively correlated with all body dimensions (Table 3) and therefore served as a suitable proxy for larval body condition. Axis 1 scores differed based on the type of water mass in which larvae were collected (Fig. 6): scores were significantly lower for plume-entrained larvae than for those from shelf waters (anchovy: Mann-Whitney *U*-tests, $U = 2307$, $p < 0.0001$; seatrout: $U = 6550$, $p < 0.0001$). Size-truncated data produced the same results (Mann-Whitney *U*-tests, $U = 1278$, $p = 0.0001$; $U = 6256$, $p < 0.0001$, respectively).

Table 3. Correlations between nonmetric multidimensional scaling axes and the 5 striped anchovy morphometric residuals and 6 sand seatrout morphometric residuals of all measured fish larvae. Axes 1 and 2 explained 71.8 and 19.4% of the variation in body size among anchovy larvae, respectively, while Axes 1 and 2 explained 88.3 and 7.8% of the variation in body size among seatrout larvae, respectively

Morphometric	Axis 1		Axis 2	
	r	p	r	p
Striped anchovy				
Eye diameter	0.354	<0.001	−0.032	0.745
Head depth	0.691	<0.001	0.471	<0.001
Head length	0.742	<0.001	−0.607	<0.001
Depth at pelvic fin	0.737	<0.001	0.427	0.004
Dorsal depth	0.807	<0.001	0.145	0.138
Sand seatrout				
Eye diameter	0.598	<0.001	−0.192	0.009
Lower jaw length	0.784	<0.001	−0.224	0.002
Head depth	0.885	<0.001	0.157	0.034
Head length	0.846	<0.001	−0.359	<0.001
Depth at pectoral fin	0.801	<0.001	0.526	<0.001
Depth at anus	0.843	<0.001	−0.152	0.041

4. DISCUSSION

4.1. Effects of plume encounter on larval fish growth and condition

To grow, survive, and successfully recruit to juvenile and adult populations, larval fishes must capture sufficient prey and avoid predation. Here we demon-

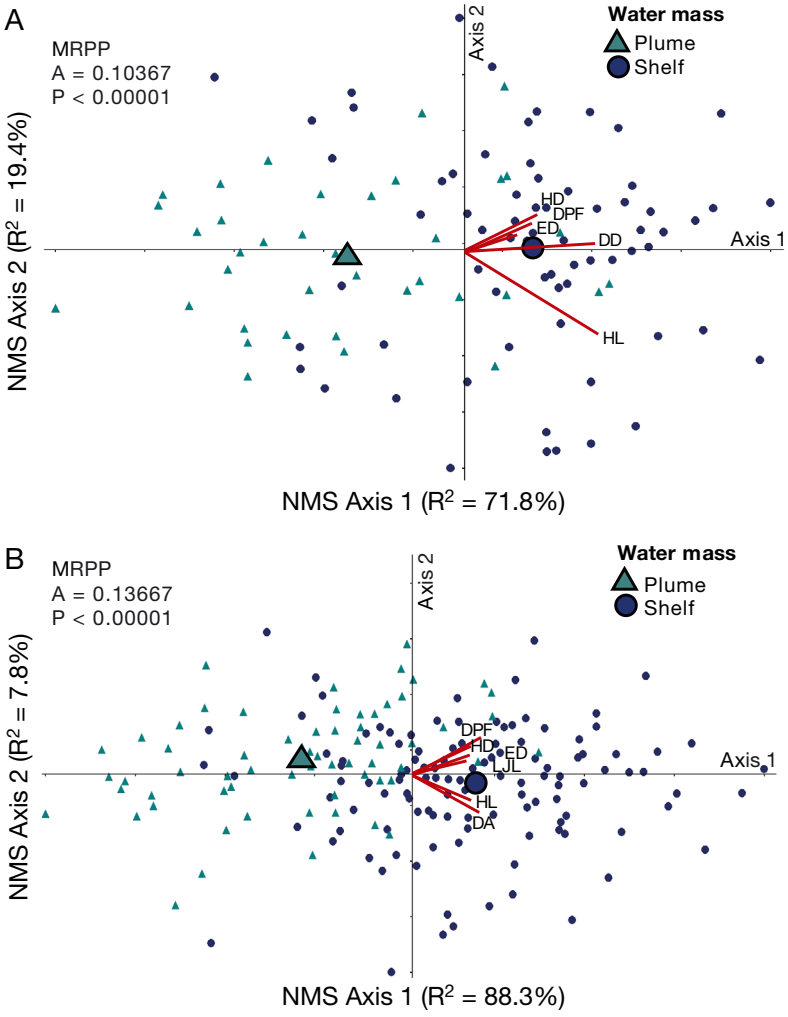

Fig. 6. Nonmetric multidimensional scaling (NMS) plots for larval (A) striped anchovy and (B) sand seatrout grouped by the type of water mass from which they were collected. Small symbols represent individual larvae collected in plume (green) and shelf (blue) water masses. Centroids for each water mass are indicated by the large symbols and represent the average position of observations in ordination space. Morphometric residuals are shown as vectors, which correspond to body depth at the pectoral fin (DPF), body depth at the anus (DA), head length (HL), head depth (HD), eye diameter (ED), and lower jaw length (LJL)

strate that despite the higher concentrations of zooplankton prey available to fish larvae, encounter with productive yet turbulent plume water exiting the mouth of Mobile Bay appears to negatively impact larval growth and condition. Otolith microstructure analyses revealed that although striped anchovy and sand seatrout larvae collected from plume and shelf water masses had similar growth rates early in life, recent growth during the last few days of life for both species was significantly lower in plume water than in adjacent coastal shelf water. While our findings are consistent with a number of previous studies that similarly found negative relationships between high freshwater discharge and the condition, growth, and survival of some larval and juvenile fishes (Deegan 1990, Day 1993, Govoni 1997, Allman & Grimes 1998, Carassou et al. 2012, Hernandez et al. 2016, Hoover 2018), other studies have found the opposite (Grimes & Lang 1992, Lang et al. 1994, Rissik & Suthers 1996). While these conflicting results in the literature may be in part taxon-specific, they also likely reflect the dynamic nature of riverine processes and reiterate the need for sampling systems that can adequately capture these fine-scale physical and biological dynamics.

Daily growth analyses may offer some insights into the timing of larval entrainment in water masses. For instance, plume-collected larval seatrout had a slower growth rate than their shelf counterparts starting quite early in life (~5–6 d), while plume-collected larval anchovies began growing significantly more slowly than their shelf conspecifics only later in life (~25 d). These diverging growth trajectories may be indicative of early encounter with turbulent, plume water for sciaenid larvae and later encounter for engraulid larvae. However, the physical or biological mechanisms leading to such potential differences in the timing of larval encounter with plume water masses are beyond the scope of the present study. Our data also suggest that once entrained within a plume, larvae are frequently retained within that water mass. If regular exchange between the 2 physical environments was occurring, daily growth trajectories would have been similar throughout the entire lifespan of the larvae, regardless of the water mass from which they were collected. Even if there was some larval movement between plume and shelf water masses, our results indicate that growth of plume-associated larvae was significantly reduced. In other words, fish larvae that spent some time in turbulent, low-salinity water grew significantly slower than fish larvae collected from more stable shelf waters. Furthermore, both species collected from plume waters were in poorer morphometric condition (e.g. skinnier at length) than their shelf counterparts. Together, these results demonstrate that larval growth and condition are affected by plume dynamics and that there are biological consequences to these encounters. In general, fast-growing fish larvae are in better condition, accumulating more lipids and reaching the minimum condition needed for metamorphosis sooner than their slower-growing counterparts (Searcy & Sponaugle 2000). Thus, the slower-growing, poorer-condition larvae in plume waters were likely more susceptible to predation. By reducing growth and lengthening the duration of the small and vulnerable larval stage (stage duration hypothesis; Anderson 1988, Cushing 1990), encounter with dynamic plume waters likely confers a survival disadvantage to fish larvae.

The present study documented a variety of potentially stressful environmental conditions inherent in plume water that could explain the observed growth and condition differences between plume and shelf-captured larval fishes. For instance, the relatively sharp interface between the brackish plume layer at the surface and salty shelf layer at the bottom could present an osmoregulatory barrier for certain fish larvae. Little is known about larval osmoregulatory physiology relative to adult and juvenile fishes, but it is possible that plume entrainment may inhibit the ability of fish larvae to maintain homeostasis, which could increase energetic demands and ultimately impact nutritional condition in addition to feeding success and growth. In an open ocean system, reef fish larvae that encountered low-salinity North Brazil Current rings for at least 7 d experienced slower growth rates than those that did not encounter these features (Sponaugle & Pinkard 2004). In the present study, salinities of 25 or less signaled the influx of a brackish plume onto the Alabama continental shelf, yet field studies in the northern Gulf of Mexico have observed larvae of both species inhabiting a wide range of salinities (sand seatrout: 0–30 salinity, Warren & Sutter 1982; striped anchovy: 0.3–44 salinity, Roessler 1970, Tarver & Savoie 1976). Temperature has been shown to heavily impact growth rates of fish larvae (Houde 1989); however, there was little difference between the mean temperature of the plume (20.8°C) and shelf stations (20.3°C). Striped anchovy larvae have previously been collected from waters ranging from 15.0 to 34.9°C (Perret 1971, Tarver & Savoie 1976), and sand seatrout larvae have been found to be abundant in water temperatures between 20 and 30°C (Warren & Sutter 1982). The relationship between low-salinity water masses and poor larval

growth and condition in our study is noteworthy, but given the eurythermal and euryhaline nature of both striped anchovy and sand seatrout, it is likely that other physical and biological factors are more directly associated with reduced larval growth and condition.

Our study revealed differences in the distribution of calanoid copepods, a major prey item for both striped anchovy and sand seatrout (McNeil & Grimes 1995, Holt & Holt 2000, Axler 2019), between plume and shelf water masses. Unfortunately, small sample sizes for both striped anchovy and sand seatrout precluded our ability to examine more than one 'control' (shelf) station using the BIONESS net data; however, *in situ* imaging enabled an examination of the prey availability in each water mass at much higher spatiotemporal resolution than traditional nets. These ISIIS data demonstrate that over the course of the study period, calanoid copepods were consistently found in higher concentrations in plume waters than in shelf waters. The higher prey supply in plume waters suggests better foraging conditions; however, spatial overlap does not imply higher feeding success as exemplified by the fact that plume larvae were growing more slowly and were in poorer condition. We therefore hypothesize that these differences in larval fish growth and condition were due to physical properties of the plume disrupting larval fish access to prey.

4.2. Access to prey in plume-influenced environments

Constraints to larval fish feeding can be imposed by aspects of the physical environment. For instance, key factors regulating the rates of larval fish feeding include turbulence, which can alter the distribution of prey with respect to their larval fish predators, and light intensity, which is linked to turbidity and suspended sediment loads, and can significantly affect visual acuity of predators (Peck et al. 2012). Turbulence dissipation rates within plume waters were an order of magnitude higher than in the ambient shelf waters, and even then, these plume turbulence values were likely higher than those measured due to the inability of the Chameleon microstructure profiler to sample the upper 4 m of the water column (see Section 2.1). While small-scale turbulence induced by wind-mixing has been observed to enhance encounter rates between fish larvae and their prey, especially at low prey concentrations (Rothschild & Osborn 1988, MacKenzie & Leggett 1991, Kristiansen et al. 2014), other studies have shown that very high levels of turbulence can reduce larval fish prey capture success due to the dispersal of aggregated prey that normally persist under more stable conditions (e.g. Lasker 1975, 1981, Kiørboe & Saiz 1995, Greer et al. 2014, Axler et al. 2020). For instance, herring larvae (Munk & Kiørboe 1985) and cod larvae (MacKenzie et al. 1994) were observed to experience declines in prey capture success at very high turbulence intensities ($\varepsilon > 10^{-1}$ cm^2 s^{-3}). Fish larvae in proximity to the Mobile Bay plume experienced turbulence intensities averaging 10^{-2} cm^2 s^{-3} (~1 × 10^{-6} W kg^{-1} turbulence dissipation rate) but reaching 10^{0} cm^2 s^{-3} (1 × 10^{-4} W kg^{-1}) in localized regions on 10–11 April 2016 (Axler et al. 2020). Further, as turbulence intensity in the water column increased, fish larvae were observed to become less spatially correlated with their calanoid copepod prey over very short time scales (Axler et al. 2020). Such high levels of turbulence appear to have reduced prey capture efficiency and feeding success, leading to the observed slower growth and poorer body condition of plume larvae.

Plume-entrained larvae may also experience diminished prey-capture abilities due to the reduction in visibility that occurs under conditions of high primary and secondary production and suspended sediments. Fish larvae are visual predators (Blaxter 1975) and need sufficient visibility to target their prey (Blaxter 1986). Therefore, turbidity can negatively affect larval feeding success by reducing reactive distance and prey contrast (Barrett et al. 1992, Gregory & Northcote 1993, Salonen et al. 2009). Mobile Bay plume water is heavily laden with suspended solids and chlorophyll (Zhao et al. 2011), 2 properties that scatter and absorb light, restricting larval fish vision (Chesney 1989). Side-by-side ISIIS images from the Mobile Bay plume and nearby coastal shelf waters during our study period illustrate how dark and full of particulates the plume is at the scale of individual fish larvae (Fig. 7). High levels of turbidity and resulting low light levels within the Mobile Bay plume could inhibit the ability of fish larvae to visually detect prey, which may have contributed to the slower growth and poorer condition of plume larvae. Gilbert et al. (1992) observed sand lance (*Ammodytes* sp.) to completely stop feeding in response to a pulse of freshwater from the Great Whale River plume in Hudson Bay. The authors attributed this to high light attenuation by the turbid waters of the expanding plume. Once vertical mixing of the plume allowed enough light to penetrate at depth, sand lance resumed feeding. Controlled experiments that meas-

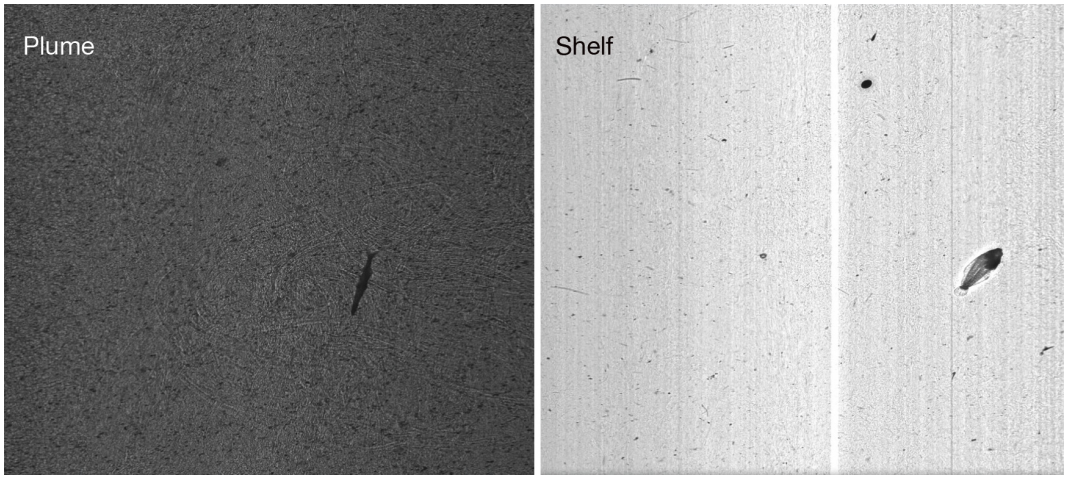

Fig. 7. Raw (uncorrected) shadowgraph images from the ISIIS showing fish larvae located in the highly turbid Mobile Bay plume water and comparatively less turbid Alabama continental shelf water. Despite the plume being a darker and noisier environment due to high particulate loads in river plumes (e.g. suspended sediments, phytoplankton), the silhouette of a clupeid fish larva is still visible

ure larval fish feeding success in response to high turbidity, turbulence, and a combination of the two are needed to be able to tease apart their effects on larval growth and condition.

4.3. Larval survivorship and ontogenetic migration in plume environments

There were clear differences in the size structure of fish larvae in this study, with populations of plume-collected fish showing a truncated distribution that lacked larger individuals compared to shelf fish. Size- and age-frequency distributions revealed that relatively larger (>15 mm) and older (>37 d) anchovy larvae and seatrout larvae (>3.5 mm and >16 d) present in shelf waters were absent from plume waters. One explanation for this difference in size and age structure could be higher predation and mortality within the plume. Research on striped anchovies across the Mississippi River outflow has suggested that natural mortality in the front (0.13 d^{-1}) and plume (0.23 d^{-1}) may be higher than that experienced in shelf waters (0.09 d^{-1}; Day 1993). In our study, slower growth in plume waters may also make fish larvae more susceptible to starvation and predation mortality, and could explain the absence of larger, older larvae in plume waters. Under stable conditions, ISIIS imagery revealed that fish larvae were significantly spatially correlated with gelatinous zooplankton predators (e.g. ctenophores, hydromedusae, and siphonophores), but not so once turbulence intensity and mixing increased (Axler et al. 2020). Therefore, a tradeoff may exist where in highly turbulent plume waters, starvation is a stronger source of mortality than losses due to predation, but the reverse is the case in more environmentally stable conditions.

Ontogenetic migration could also explain the observed differences in larval fish size and age structure between plume and shelf waters. The absence of larger and older larvae from plume waters may indicate that at a certain size and age (~16 mm for anchovies and ~4 mm for seatrout), fish larvae may be sufficiently developed (post-flexion) to actively avoid these unfavorable habitats, instead aggregating along the plume frontal regions and ambient shelf waters. In this case, successful plume avoidance would entail overcoming the strong currents and turbulence and swimming either horizontally or vertically out of or away from the plume water mass, potentially by taking advantage of favorable ambient currents that reduce dispersive losses (Paris & Cowen 2004). Similar patterns in size frequency distributions of larval blue crab *Callinectes sapidus* were found in the Delaware Bay plume (Tilburg et al. 2009). While patches of earlier-stage crab larvae were dispersed throughout the main body of the plume, later-stage, older blue crab larvae occurred almost entirely in the higher salinities of the frontal region and ambient ocean. In our study, the fact that plume-entrained fish larvae were comparatively smaller and in poorer condition than their shelf counterparts suggests that these larvae (many pre-flexion) may have been too small or weak to avoid or escape from the strong plume currents and were therefore dispersed throughout the main body of the plume.

Published swimming speeds of striped anchovy and sand seatrout larvae are unavailable; however, swimming speeds of closely related species suggest that escape from the strong plume currents by pre-flexion larvae is unlikely. For instance, temperate and tropical sciaenid larvae have been recorded to swim at critical speeds (U_{crit}) of 1.1–20.5 cm s^{-1} (e.g. *Sciaenops ocellatus*, 3.0–23.4 mm SL; Fuiman et al. 1999) and *in situ* speeds of 2.5–8.4 cm s^{-1} (e.g. *Argyrosomus japonicus*, 3.5–14.0 mm SL; Clark et al. 2005). Temperate engraulids have routine swimming speeds of 1.0–20.0 cm s^{-1} (e.g. *Engraulis mordax*, 4.0–25.1 mm SL; Hunter 1972). In comparison, current velocities within the Mobile Bay plume reached 50 cm s^{-1} during peak flows. Therefore, it seems unlikely that pre-flexion sand seatrout (<4 mm) or striped anchovies (<10 mm) entrained within the plume would have been able to overcome the swift currents. Outside of the plume, ambient currents moved shoreward at 10–25 cm s^{-1}, which is more typical of the coastal region and could enhance retention of fish larvae in these nearshore regions.

In short, it is likely that a combination of physical forcing and ontogenetic swimming behavior facilitates transport and retention of fish larvae in these river-dominated ecosystems. Fish larvae distributed near a plume may respond variably depending on ontogeny such that the early stages (pre-flexion) are entrained and advected more easily while larger, older larvae are able to maintain their position near highly productive estuaries by taking advantage of ambient shoreward currents (Epifanio 1988, Teodósio et al. 2016).

5. CONCLUSIONS

In coastal river-dominated ecosystems, a variety of hydrological processes and environmental conditions can impact survival of the early life stages of coastal fishes, but few studies have been able to characterize the plume environment at sufficiently fine scales to resolve the underlying mechanisms. Coupling high-resolution environmental sampling of a 2-layer river–estuarine system with otolith and morphometric analyses over the same time period enabled the examination of the effects of plume encounter on larval fish growth and condition at very fine spatial and temporal scales. These data revealed that fish larvae within a coastal plume could experience increased prey contact due to the elevated zooplankton biomass aggregated within the productive feature; however, higher spatial co-occurrence of fish larvae with zooplankton prey did not translate to higher feeding success. Despite the seemingly abundant feeding opportunities within the plume, fish larvae grew more slowly and were skinnier-at-length than their shelf (non-plume) conspecifics. We hypothesize that these differences in growth and condition are attributable to the physical and/or visual impairment of larval fish feeding due to the dynamic physical properties inherent of plume water masses (i.e. increased turbulence and turbidity relative to the surrounding coastal waters), which result in measurable biological consequences.

Future climate predictions for the northern Gulf of Mexico include elevated river discharge due to heavy precipitation from storms and run-off (Coumou & Rahmstorf 2012). The increase in frequency, magnitude, and duration of freshwater delivered to coastal ecosystems may have few direct negative effects on many coastal fish species due to their relatively high tolerance of fluctuations in both salinity and temperature (e.g. Tytler & Bell 1989). While increased nutrient-rich river discharge would enhance coastal primary productivity, early life stages may not benefit from this higher productivity. Because fish larvae are visual predators, highly turbid waters, characteristic of plumes, could impair the ability of fish larvae to forage successfully despite the higher zooplankton biomass accompanying enhanced primary productivity. Further, higher river discharge and widespread turbulent frontal zones may inhibit the prey capture abilities of entrained fish larvae. Ultimately, results of the present study build on our understanding of how increased river discharge worldwide can influence nearshore marine fish communities at scales relevant to the vulnerable larval stages.

Acknowledgements. We thank the captains and crews of RVs 'Point Sur' and 'Pelican' for their assistance during the CONCORDE field sampling campaigns. Thanks also to numerous PIs, post-docs, technicians, and graduate students for their involvement with CONCORDE cruise logistics, field data collection, and sample processing, especially A. Deary, O. Lestrade, A. Hoover, S. Muffelman, K. Heidenreich, A. Greer, C. Zapfe, M. Angelina, J. Herrmann, A. Boyette, and K. Martin. Special thanks to E. Haffey for identifying ichthyoplankton and to C. Gavins for identifying zooplankton. Guidance was provided by K. Shulzitski and E. Goldstein for otolith microstructure analyses, and data analyses were enhanced by discussions with M. Gleiber and H. Fennie. This research was made possible by a grant from the Gulf of Mexico Research Initiative and is contribution EcoFOCI-0945 to NOAA's Ecosystems and Fisheries-Oceanography Coordinated Investigations Program. Raw collection data are available through the Gulf of Mexico Research Initiative Information & Data Cooperative (GRIIDC) at https://data.gulfresearchinitiative.org (BIONESS

ichthyoplankton data: https://doi.org/10.7266/4VG6WW99, ISIIS zooplankton data: https://doi.org/10.7266/9211C8TM, larval striped anchovy and sand seatrout growth and condition data: https://doi.org/10.7266/M4ZEFDZY).

LITERATURE CITED

Allman RJ, Grimes CB (1998) Growth and mortality of little tunny (*Euthynnus alletferatus*) larvae off the Mississippi River plume and Panama City, Florida. Bull Mar Sci 62: 189–197

Anderson JT (1988) A review of size dependent survival during pre-recruit stages of fishes in relation to recruitment. J Northwest Atl Fish Sci 8:55–66

Axler KE (2019) Influence of river plumes on larval fish distributions, predator–prey relationships, and fitness in the northern Gulf of Mexico. MSc thesis, Oregon State University, Corvallis, OR

Axler KE, Sponaugle S, Briseño-Avena C, Hernandez F Jr and others (2020) Fine-scale larval fish distributions and predator–prey dynamics in a coastal river-dominated ecosystem. Mar Ecol Prog Ser 650:37–61

Barrett JC, Grossman GD, Rosenfeld J (1992) Turbidity-induced changes in reactive distance of rainbow trout. Trans Am Fish Soc 121:437–443

Baumann H, Pepin P, Davidson FJ, Mowbray F, Schnack D, Dower JF (2003) Reconstruction of environmental histories to investigate patterns of larval radiated shanny (*Ulvaria subbifurcata*) growth and selective survival in a large bay of Newfoundland. ICES J Mar Sci 60:243–258

Blaxter JHS (1963) The feeding of herring larvae and their ecology in relation to feeding. Calif Coop Ocean Fish Invest Rep 10:79–88

Blaxter JHS (1975) The eyes of larval fish. In: Ali MA (ed) Vision in fishes. Plenum Publishing, New York, NY, p 757–773

Blaxter JHS (1986) Development of sense organs and behavior of teleost larvae with special reference to feeding and predator avoidance. Trans Am Fish Soc 115:98–114

Burnham KP, Anderson DR, Burnham KP (2002) Model selection and multimodel inference: a practical information-theoretic approach. Springer, New York, NY

Carassou L, Hernandez FJ, Powers SP, Graham WM (2012) Cross-shore, seasonal, and depth-related structure of ichthyoplankton assemblages in coastal Alabama. Trans Am Fish Soc 141:1137–1150

Checkley DM Jr (1982) Selective feeding by Atlantic herring (*Clupea harengus*) larvae on zooplankton in natural assemblages. Mar Ecol Prog Ser 9:245–253

Chesney EJ Jr (1989) Estimating the food requirements of striped bass larvae *Morone saxatilis*: effects of light, turbidity and turbulence. Mar Ecol Prog Ser 53:191–200

Clark DL, Leis JM, Hay AC, Trnski T (2005) Swimming ontogeny of larvae of four temperate marine fishes. Mar Ecol Prog Ser 292:287–300

Coumou D, Rahmstorf S (2012) A decade of weather extremes. Nat Clim Chang 2:491–496

Cowan JH, Grimes CB, Shaw RF (2008) Life history, history, hysteresis, and habitat changes in Louisiana's coastal ecosystem. Bull Mar Sci 83:197–215

Cowen RK, Guigand CM (2008) *In Situ* Ichthyoplankton Imaging System (ISIIS): system design and preliminary results. Limnol Oceanogr Methods 6:126–132

Cowen RK, Greer AT, Guigand CM, Hare JA, Richardson DE, Walsh HJ (2013) Evaluation of the *In Situ* Ichthyoplankton Imaging System (ISIIS): comparison with the traditional (bongo net) sampler. Fish Bull 111:1–12

Cushing DH (1990) Plankton production and year-class strength in fish populations: an update of the match/mismatch hypothesis. Adv Mar Biol 26:249–293

Day GR (1993) Distribution, abundance, growth and mortality of striped anchovy, *Anchoa hepsetus*, about the discharge plume of the Mississippi River. MSc thesis, University of West Florida, Pensacola, FL

Deegan LA (1990) Effects of estuarine environmental conditions on population dynamics of young-of-the-year gulf menhaden. Mar Ecol Prog Ser 68:195–205

Dinnel SP, Schroeder WW, Wiseman WJ Jr (1990) Estuarine-shelf exchange using Landsat images of discharge plumes. J Coast Res 6:789–799

Dzwonkowski B, Park K, Lee J, Webb BM, Valle-Levinson A (2014) Spatial variability of flow over a river-influenced inner shelf in coastal Alabama during spring. Cont Shelf Res 74:25–34

Epifanio CE (1988) Transport of crab larvae between estuaries and the continental shelf. In: Jansson BO (ed) Coastal–offshore ecosystem interactions. Lecture Notes on Coastal and Estuarine Studies, Vol 22. Springer, Berlin, p 291–305

Fuiman LA, Smith ME, Malley VN (1999) Ontogeny of routine swimming speed and startle responses in red drum, with a comparison of responses to acoustic and visual stimuli. J Fish Biol 55:215–226

Gilbert M, Fortier L, Ponton D, Drolet R (1992) Feeding ecology of marine fish larvae across the Great Whale River plume in seasonally ice-covered southeastern Hudson Bay. Mar Ecol Prog Ser 84:19–30

Gisbert E, Conklin D, Piedrahita R (2004) Effects of delayed first feeding on the nutritional condition and mortality of California halibut. J Fish Biol 64:116–132

Govoni JJ (1997) The association of the population recruitment of gulf menhaden, *Brevoortia patronus*, with Mississippi River discharge. J Mar Syst 12:101–108

Govoni JJ, Chester AJ (1990) Diet composition of larval *Leiostomus xanthurus* in and about the Mississippi River plume. J Plankton Res 12:819–830

Govoni JJ, Grimes CB (1992) The surface accumulation of larval fishes by hydrodynamic convergence within the Mississippi River plume front. Cont Shelf Res 12: 1265–1276

Greer AT, Cowen RK, Guigand CM, Hare JA, Tang D (2014) The role of internal waves in larval fish interactions with potential predators and prey. Prog Oceanogr 127:47–61

Greer AT, Shiller AM, Hofmann EE, Wiggert JD and others (2018) Functioning of coastal river-dominated ecosystems and implications for oil spill response. Oceanography 31:90–103

Gregory RS, Northcote TG (1993) Surface, planktonic, and benthic foraging by juvenile chinook salmon (*Oncorhynchus tshawytscha*) in turbid laboratory conditions. Can J Fish Aquat Sci 50:223–240

Grimes CB, Finucane JH (1991) Spatial distribution and abundance of larval and juvenile fish, chlorophyll and macrozooplankton around the Mississippi River discharge plume, and the role of the plume in fish recruitment. Mar Ecol Prog Ser 75:109–119

Grimes CB, Kingsford MJ (1996) How do riverine plumes of different sizes influence fish larvae: Do they enhance recruitment? Mar Freshw Res 47:191–208

Grimes CB, Lang KL (1992) Distribution, abundance, growth, mortality, and spawning dates of yellowfin tuna, *Thun-*

nus albacares, larvae around the Mississippi River discharge plume. Collect Vol Sci Pap ICCAT Recl Doc Sci 38:177–194

Grorud-Colvert K, Sponaugle S (2006) Influence of condition on behavior and survival potential of a newly settled coral reef fish, the bluehead wrasse *Thalassoma bifasciatum.* Mar Ecol Prog Ser 327:279–288

Hernandez FJ Jr, Filbrun JE, Fang J, Ransom JT (2016) Condition of larval red snapper (*Lutjanus campechanus*) relative to environmental variability and the Deepwater Horizon oil spill. Environ Res Lett 11:094019

Holt GJ, Holt SA (2000) Vertical distribution and the role of physical processes in the feeding dynamics of two larval sciaenids *Sciaenops ocellatus* and *Cynoscion nebulosus.* Mar Ecol Prog Ser 193:181–190

Hoover AM (2018) Influence of natural and anthropogenic environmental variability on larval fish diet, growth, and condition in the northcentral Gulf of Mexico. MSc thesis, University of Southern Mississippi, Hattiesburg, MS

Houde ED (1987) Fish early life dynamics and recruitment variability. Am Fish Soc Symp 2:17–29

Houde ED (1989) Subtleties and episodes in the early life of fishes. J Fish Biol 35:29–38

Houde ED (2009) Recruitment variability. In: Jakobsen T, Fogarty BA, Megrey BA, Moksness E (eds) Fish reproductive biology: implications for assessment and management. Wiley-Blackwell, Chichester, p 91–171

Hunter J (1972) Swimming and feeding behavior of larval anchovy *Engraulis mordax.* Fish Bull 70:821–838

Kingsford MJ, Suthers IM (1994) Dynamic estuarine plumes and fronts: importance to small fish and plankton in coastal waters of NSW, Australia. Cont Shelf Res 14:655–672

Kiørboe T, Saiz E (1995) Planktivorous feeding in calm and turbulent environments, with emphasis on copepods. Mar Ecol Prog Ser 122:135–145

Kristiansen T, Vollset KW, Sundby S, Vikebø F (2014) Turbulence enhances feeding of larval cod at low prey densities. ICES J Mar Sci 71:2515–2529

Kruskal JB (1964) Nonmetric multidimensional scaling: a numerical method. Psychometrika 29:115–129

Lang KL, Grimes CB, Shaw RF (1994) Variations in the age and growth of yellowfin tuna larvae, *Thunnus albacares*, collected about the Mississippi River plume. Environ Biol Fishes 39:259–270

Lasker R (1975) Field criteria for survival of anchovy larvae: the relation between inshore chlorophyll maximum layers and successful first feeding. Fish Bull 73:453–462

Lasker R (1981) The role of a stable ocean in larval fish survival and subsequent recruitment. In: Lasker R (ed) Marine fish larvae: morphology, ecology and relation to fisheries. University of Washington Press, Seattle, WA, p 80–87

Le Fèvre J (1987) Aspects of the biology of frontal systems. Adv Mar Biol 23:163–299

Lochmann SE, Ludwig G (2003) Relative triacylglycerol and morphometric measures of condition in sunshine bass fry. N Am J Aquacult 65:191–202

Lochmann SE, Taggart CT, Griffin DA, Thompson KR, Maillet GL (1997) Abundance and condition of larval cod (*Gadus morhua*) at a convergent front on Western Bank, Scotian Shelf. Can J Fish Aquat Sci 54:1461–1479

Lohrenz SE, Fahnenstiel GL, Redalje DG, Lang GA, Chen X, Dagg MJ (1997) Variations in primary production of northern Gulf of Mexico continental shelf waters linked to nutrient inputs from the Mississippi River. Mar Ecol Prog Ser 155:45–54

MacKenzie BR, Leggett WC (1991) Quantifying the contribution of small-scale turbulence to the encounter rates between larval fish and their zooplankton prey: effects of wind and tide. Mar Ecol Prog Ser 73:149–160

MacKenzie BR, Miller TJ, Cyr S, Leggett WC (1994) Evidence for a dome-shaped relationship between turbulence and larval fish ingestion rates. Limnol Oceanogr 39:1790–1799

Mather PM (1976) Computational methods of multivariate analysis in physical geography. Wiley, New York, NY

McCune B, Grace JB, Urban DL (2002) Analysis of ecological communities, Vol 28. MjM Software Design, Gleneden Beach, OR

McNeil CS, Grimes CB (1995) Diet and feeding ecology of striped anchovy, *Anchoa hepsetus*, along environmental gradients associated with the Mississippi River discharge plume. In: Atwood DK, Graham WF, Grimes CB (eds) Nutrient-enhanced coastal ocean productivity. Proceedings of the April 1994 Synthesis Workshop, Baton Rouge, Louisiana. Louisiana Sea Grant College Program, Baton Rouge, LA, p 81–89

Morgan CA, De Robertis A, Zabel RW (2005) Columbia River plume fronts. I. Hydrography, zooplankton distribution, and community composition. Mar Ecol Prog Ser 299:19–31

Moum JN, Gregg MC, Lien RC, Carr ME (1995) Comparison of turbulence kinetic energy dissipation rate estimates from two ocean microstructure profilers. J Atmos Ocean Technol 12:346–366

Munk P, Kiørboe T (1985) Feeding behaviour and swimming activity of larval herring (*Clupea harengus*) in relation to density of copepod nauplii. Mar Ecol Prog Ser 24:15–21

Paris CB, Cowen RK (2004) Direct evidence of a biophysical retention mechanism for coral reef fish larvae. Limnol Oceanogr 49:1964–1979

Peck MA, Huebert KB, Llopiz JK (2012) Intrinsic and extrinsic factors driving match-mismatch dynamics during the early life history of marine fishes. Adv Ecol Res 47: 177–302

Perret WS (1971) Cooperative Gulf of Mexico estuarine inventory and study, Louisiana — Phase IV, Biology. Louisiana Wildlife and Fisheries Commission, New Orleans, LA, p 31–69

Peterson JO, Peterson WT (2008) Influence of the Columbia River plume (USA) on the vertical and horizontal distribution of mesozooplankton over the Washington and Oregon shelf. ICES J Mar Sci 65:477–483

Pinheiro J, Bates D, DebRoy S, Satkar D, R Core Team (2019) nlme: Linear and nonlinear mixed effects models. R package version 3.1-141. https://CRAN.R-project.org/package=nlme

Powell AB, Chester AJ, Govoni JJ, Warlen SM (1990) Nutritional condition of spot larvae associated with the Mississippi River plume. Trans Am Fish Soc 119:957–965

Pryor VK, Epifano CE (1993) Prey selection by larval weakfish (*Cynoscion regalis*): the effects of prey size, speed, and abundance. Mar Biol 116:31–37

Core Team (2019) R: a language and environment for statistical computing. R Foundation for Statistical Computing, Vienna

Ransom JT, Filbrun JE, Hernandez FJ Jr (2016) Condition of larval Spanish mackerel *Scomberomorus maculatus* in relation to the *Deepwater Horizon* oil spill. Mar Ecol Prog Ser 558:143–152

Rettig J, Shuman L, McCloskey J (2006) Seasonal patterns of abundance: Do zooplankton in small ponds do the same thing every spring–summer? Hydrobiologia 556:193–207

Richards WJ (2005) Early stages of Atlantic fishes. CRC Press, Boca Raton, FL

Rissik D, Suthers IM (1996) Feeding in a larval fish assemblage: the nutritional significance of an estuarine plume front. Mar Biol 125:233–240

Robert D, Castonguay M, Fortier L (2009) Effects of preferred prey density and temperature on feeding success and recent growth in larval mackerel of the southern Gulf of St. Lawrence. Mar Ecol Prog Ser 377:227–237

Roessler MA (1970) Checklist of fishes in Buttonwood Canal, Everglades National Park, Florida, and observations on the seasonal occurrence and life histories of selected species. Bull Mar Sci 20:860–890

Rothschild BJ, Osborn TR (1988) Small-scale turbulence and plankton contact rates. J Plankton Res 10:465–474

Sabatés A, Masó M (1990) Effect of a shelf-slope front on the spatial distribution of mesopelagic fish larvae in the western Mediterranean. Deep-Sea Res A Oceanogr Res Pap 37:1085–1098

Salonen M, Urho L, Engström-Öst J (2009) Effects of turbidity and zooplankton availability on the condition and prey selection of pike larvae. Boreal Environ Res 14:981–989

Schroeder WW, Lysinger WR (1979) Hydrography and circulation in Mobile Bay. In: Loyacano HA, Smith JP (eds) Symposium on the natural resources of the Mobile Bay Estuary. U.S. Army Corps of Engineers, Mobile, AL, p 75–94

Searcy SP, Sponaugle S (2000) Variable larval growth in a coral reef fish. Mar Ecol Prog Ser 206:213–226

Sponaugle S, Pinkard DR (2004) Impact of variable pelagic environments on natural larval growth and recruitment of the reef fish *Thalassoma bifasciatum.* J Fish Biol 64: 34–54

Sponaugle S, Llopiz JK, Havel LN, Rankin TL (2009) Spatial variation in larval growth and gut fullness in a coral reef fish. Mar Ecol Prog Ser 383:239–249

Suthers IM (1998) Bigger? Fatter? Or is faster growth better? Considerations on condition in larval and juvenile coral-reef fish. Austral Ecol 23:265–273

Tarver JW, Savoie LR (1976) An inventory and study of the Lake Pontchartrain-Lake Maurepas estuarine complex - Phase 11, Biology. Tech Bull 19. Louisiana Wildlife and Fisheries Commission, Oysters, Water Bottoms, and Seafoods Division, p 7–99

Teodósio MA, Paris CB, Wolanski E, Morais P (2016) Biophysical processes leading to the ingress of temperate fish larvae into estuarine nursery areas: a review. Estuar Coast Sci 183:187–202

Tilburg CE, Dittel AI, Epifanio CE (2009) High concentrations of crab larvae along the offshore edge of a coastal current: effects of convergent circulation. Fish Oceanogr 18:135–146

Tytler P, Bell MV (1989) A study of diffusional permeability of water, sodium, and chloride in marine fish larvae. J Exp Biol 147:125–132

Uye SI, Yamaoka T, Fujisawa T (1992) Are tidal fronts good recruitment areas for herbivorous copepods? Fish Oceanogr 1:216–226

Warren JR, Sutter FC (1982) Industrial bottomfish-monitoring and assessment. In: Fishery Monitoring and Assessment Completion Report, 1 January 1977 to 31 December 1981, Ch. II, Sec. I, Proj. No. 2-296-R. Gulf Coast Research Laboratory, Ocean Springs, MS, p 43–69

Weisberg S, Spangler G, Richmond LS (2010) Mixed effects models for fish growth. Can J Fish Aquat Sci 67:269–277

Wickham H (2016) Ggplot2: elegant graphics for data analysis. Springer-Verlag, New York, NY

Wickham H, François R, Henry L, Müller K (2018) Dplyr: a grammar of data manipulation. R package version 0.7.6. https://CRAN.R-project.org/package=dplyr

Zhao H, Chen Q, Walker ND, Zheng Q, Macintyre HL (2011) A study of sediment transport in a shallow estuary using MODIS imagery and particle tracking simulation. Int J Remote Sens 32:6653–6671

Editorial responsibility: Rebecca Asch (Guest Editor), Greenville, NC, USA

Submitted: October 17, 2019; Accepted: June 23, 2020
Proofs received from author(s): July 27, 2020